crystals

MDPI

Article

# Fast Turn-Off Switching of Vertically-Aligned Negative Liquid Crystals by Fine Patterning of Pixel Electrodes

**Yeongyu Choi, Tae-Hoon Choi, Jae-Hyeon Woo, Byoung-Gyu Jeon and Tae-Hoon Yoon** *

Department of Electronics Engineering, Pusan National University, Busan 46241, Korea; choiyg@pusan.ac.kr (Y.C.); thchoi@pusan.ac.kr (T.-H.C.); woojae@pusan.ac.kr (J.-H.W.); wjs5538@pusan.ac.kr (B.-G.J.)

* Correspondence: thyoon@pusan.ac.kr

Academic Editor: Wei Lee

Received: 25 May 2017; Accepted: 30 June 2017; Published: 3 July 2017

**Abstract:** We investigated the two-dimensional (2D) confinement effect on the switching of vertically-aligned negative liquid crystals (LCs) by an electric field applied between the top and bottom patterned electrodes. When an electric field is applied to a patterned vertical alignment (PVA) cell, virtual walls form in the middle of the gaps between and at the center of the patterned electrodes. These virtual walls formed in a PVA cell results in the turn-off time being dependent on the pitch of the patterned electrodes as well as the cell gap. We found that a short response time can be achieved by the fine patterning of pixel electrodes with little decrease in the transmittance. The obtained numerical results agree well with the model based on the 2D confinement effect of LCs.

**Keywords:** liquid crystals; liquid crystal device; fast switching; 2D confinement

## 1. Introduction

Currently, liquid crystal displays (LCDs) are competing with organic light-emitting diodes (OLEDs) in the flat-panel display market because each display technology has its pros and cons. LCDs have been widely used in various electronic devices because of their superior performance, such as higher pixel density, larger panel size, lower power consumption, and longer lifetime compared to OLEDs [1–3]. Nevertheless, some technical barriers still remain, such as the narrow viewing angle, low contrast ratio, poor color gamut, and relatively slow response. The range of viewing angles could be expanded by using compensation films and multidomain structures, and a high contrast ratio over 100,000:1 could be achieved by using local dimming technologies [4,5]. Moreover, the emerging technology of quantum dots could make the LCD color gamut equivalent to or better than that of OLEDs [6]. However, the long LC response time, which causes motion blur and deteriorated image quality, remains a critical issue [4,5].

Among the various LC modes, the vertical alignment (VA) mode exhibits a superior dark state because of the initially vertically-aligned LCs, resulting in the highest contrast ratio [7]. To widen the viewing angle range in the VA mode, various multidomain structures have been proposed [8–12]. Among them, two types of multidomain structures, the multidomain VA mode [11] and patterned VA (PVA) mode [12], are widely used in large LCD devices. However, the response time of VA cells is very slow because of the high rotational viscosity of the LC material with negative dielectric anisotropy and optical bouncing caused by the backflow effect during the turn-on process. In contrast to other LC modes, the turn-on switching of VA cells is much slower than the turn-off switching because of the propagation of the LC domains. Therefore, most studies have focused on the reduction of the turn-on time rather than the turn-off time. The turn-on time of a VA cell could be greatly reduced by introducing overdrive technology [13,14] and the formation of the pretilt angle using a UV-curable prepolymer [15–17]. However, the pretilt can increase the turn-off time because the accumulated elastic energy of LCs in the turn-on state decreases with the pretilt angle. The slow turn-off switching remains a critical issue because this process relies only on the slow relaxation of LCs.

In this paper, we report the effects of two-dimensional (2D) confinement on the switching of vertically aligned negative LCs. In a PVA cell, both the top common and bottom pixel electrodes are patterned on each substrate, as shown in Figure 1a. When an electric field is applied to the LC cell, virtual walls form in the middle of the gaps between and at the center of the patterned electrodes. The LC molecules are confined not only by the two substrates but also by the virtual walls. We found that the turn-off time of a PVA cell can be reduced simply by decreasing the pitch of the patterned electrodes. In contrast to the switching of the vertically-aligned LCs with positive dielectric anisotropy by an in-plane electric field, known as the VA-IPS mode [18,19], a PVA cell using LCs with negative dielectric anisotropy exhibits little decrease in the transmittance by the fine patterning of pixel electrodes because the dead zone formed at the center of each pixel electrode is very narrow.

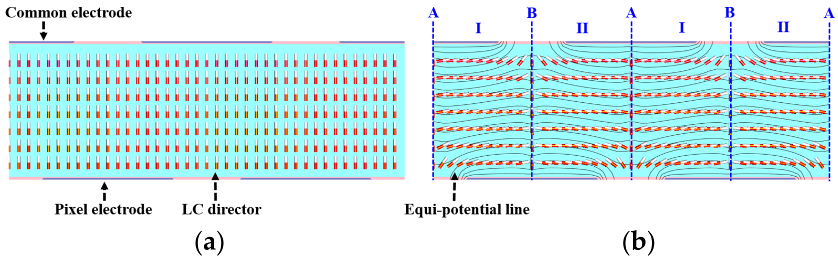


**Figure 1.** The device structure of a PVA cell with LC director configurations in the (**a**) off and (**b**) on states.

## 2. Response Time of a PVA Cell

The turn-on time of a VA cell can be reduced by employing overdriving technologies, so-called dynamic capacitance compensation (DCC I [13] and DCC II [14]) and polymer-stabilization technologies [15–17]. However, there are currently no practical solutions available for reducing the turn-off time because it is limited by the slow relaxation of LCs. As mentioned above, when an electric field is applied between the top common and bottom pixel electrodes, the LC molecules in region I tilt downward in a clockwise direction, while those in region II tilt downward in a counter-clockwise direction, as shown in Figure 1b. The LC molecules tilt downward along the diagonal direction with respect to the transmission axes of the two polarizers so that the cell switches to the bright state. At boundaries A and B between regions I and II, there is no change in the polar angle of the LC director, because the neighboring LC molecules are oriented in the opposite direction; therefore, boundaries A and B can be treated as virtual walls [19–23]. As a result, in a PVA cell, no light is transmitted at boundaries A and B, as shown in Figure 2, in contrast to single-domain VA cells, where the transmittance distribution is uniform and the incident light is transmitted over the entire cell area. In other words, the LC molecules in a PVA cell are confined in two dimensions not only by the two substrates but also by the virtual walls. A similar behavior has been observed in a VA-IPS cell using LCs with positive dielectric anisotropy [19].

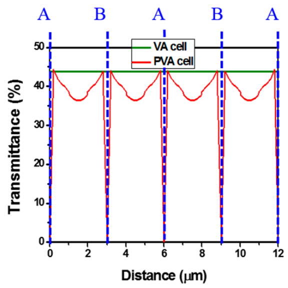


**Figure 2.** Calculated transmittance distribution in a PVA cell.

## 3. Results and Discussion

To confirm the dynamic switching behavior of the LCs in a PVA cell, the Ericksen–Leslie equation, coupled with the Laplace equation, was numerically solved using the finite element method. The Ericksen–Leslie equation has been used to describe the motion of the LC director. Numerical calculations were performed using the commercial software package TechWiz LCD 2D (Sanayi System Company, Ltd., Incheon, Korea). The LC material parameters used in the numerical calculations were as follows: splay elastic constant $K_{11}$ = 14.7 pN, twist elastic constant $K_{22}$ = 7.4 pN, bend elastic constant $K_{33}$ = 15.9 pN, optical anisotropy $\Delta n$ = 0.1096, dielectric anisotropy $\Delta\varepsilon = -3.9$, and rotational viscosity $\gamma_1$ = 110 mPa·s. The thickness of the LC layer was 3.5 μm. The pitch $P$ of the patterned electrodes varied from 6 to 16 μm. The spacing L between the patterned electrodes was fixed at 2 μm.

The turn-off time of a single-domain VA cell can be represented by the following approximated equation under the one-dimensional (1D) confinement of LCs between two substrates:

$$\tau_{off} = \frac{\gamma_1 d^2}{K_{33}\pi^2} \quad (1)$$

where $\gamma_1$ is the rotational viscosity, $d$ is the cell gap, and $K_{33}$ is the bend elastic constant. As shown in Equation (1), the turn-off time is proportional to the visco-elastic coefficient ($\gamma_1/K_{33}$) and the square of the cell gap d. In contrast to a single-domain VA cell where the LCs are confined in one dimension between the two substrates, the numerical results indicate that the turn-off time of a PVA cell is largely dependent on the pitch of the patterned electrodes, as shown by the blue dots in Figure 3. As the pitch of the patterned electrodes decreases, the turn-off time decreases. In a PVA cell, the polar angle of the LC director does not change at boundaries A and B even when an electric field is applied between the top and bottom patterned electrodes, as shown in Figure 1b. We can consider boundaries A and B as virtual walls, by which the LC molecules are confined in two dimensions not only by the two substrates but also by the virtual walls. Under the 2D confinement of LCs, the turn-off time of a PVA cell can be written as:

$$\tau_{off} = \frac{\gamma_1}{K_{33}\left(\frac{\pi}{d}\right)^2 + K_{11}\left(\frac{\pi}{P/2}\right)^2} \quad (2)$$

As shown in Equation (2), the turn-off time is dependent on the pitch $P$ of the patterned electrodes as well as the cell gap $d$. Here, the distance between the neighboring virtual walls is half of the pitch $P$ of the patterned electrodes. As the pitch of the patterned electrodes decreases, the turn-off time significantly decreases as a result of the reduced distance between neighboring virtual walls, as shown by the red line in Figure 3. The numerically calculated turn-off times obtained agree well with the 2D model, as shown in Figure 3. The turn-off time calculated by using the 2D model converges to the 1D model, as shown in Figure 3, because the 2D confinement effect will become negligible as the pitch is increased. Numerical results of a PVA cell also converges to those of a single-domain VA cell. It may be noted that the turn-off times calculated by using the 1D or 2D model do not match exactly with the numerical results.

To investigate the effect of the elastic constants on the turn-off time, we calculated the turn-off time numerically under the conditions (1) $K_{11} < K_{33}$ (LC I), (2) $K_{11} = K_{33}$ (LC II), and (3) $K_{11} > K_{33}$ (LC III). The elastic constants of each LC are shown in Table 1. Other material paramters of the LC were assumed to be the same as those used for other numerical calculations. As shown in Figure 4, the dependence of the turn-off time on the electrode pitch was rarely affected by the ratio of the elastic constants. Recently, it was reported that the turn-off time of a VA-IPS cell using LCs with positive dielectric anisotropy exhibits the same trend as a PVA cell; the turn-off time decreases when the pitch of the interdigitated electrodes decreases. In a VA-IPS cell, the electric field is not uniform in either the longitudinal or lateral direction. As a result, the turn-off time obtained with Equation (2) in a VA-IPS cell exhibits a deviation from the numerical results, and Equation (2) was modified to accurately account for the turn-off time [19]. In contrast, the turn-off time of a PVA cell matched well with the theoretical analysis based on the 2D confinement effect without any modification because of the relatively uniform electric field distribution. We will discuss this later.

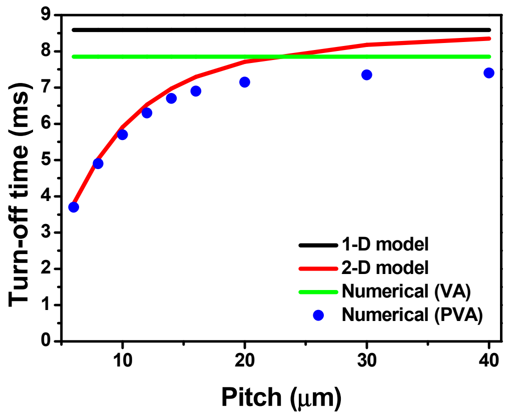


**Figure 3.** Turn-off times of PVA cells obtained using a 1D model, 2D model, and numerical calculation as a function of patterned electrodes pitch.

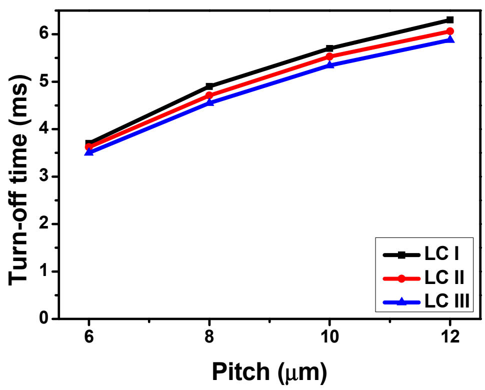


**Figure 4.** Turn-off times of PVA cells obtained using three different LC materials as a function of patterned electrodes pitch.

**Table 1.** Elastic constants of the three different LC materials used in our numerical calculation.

| | $K_{11}$ | $K_{22}$ | $K_{33}$ |
|---|---|---|---|
| LC I | 14.7 pN | 7.4 pN | 15.9 pN |
| LC II | 15.9 pN | 7.4 pN | 15.9 pN |
| LC III | 17.1 pN | 7.4 pN | 15.9 pN |

We calculated the voltage–transmittance curves and turn-off times of PVA cells with the pitch *P* of patterned electrodes as a parameter, as shown in Figure 5. A single-domain VA cell exhibits a high transmittance of 44.7% at an applied voltage of 5.1 V, as shown in Figure 5a. As the pitch of patterned electrodes decreases, the maximum transmittance of a PVA cell decreases, while both the threshold and operating voltages increase. The maximum transmittance of a PVA cell with $P$ = 16 μm is 38.9% at an applied voltage of 6.9 V, whereas that of a PVA cell with $P$ = 6 μm is 38.0% at an applied voltage of 14 V. We also calculated the temporal switching behaviors during the turn-off process, as shown in Figure 5b. We define the turn-off time as the transient time for the transmittance to decay from 90% to 10% of the maximum value. The calculated turn-off time of a single-domain VA cell was 7.85 ms, whereas the turn-off times of PVA cells with $P$ of 16 and 6 μm were 6.86 and 3.72 ms, respectively. As the pitch of the patterned electrodes decreases, the turn-off time significantly decreases, as expected by the effect of the 2D confinement with virtual walls. The turn-off switching of a PVA cell with $P$ = 6 μm is 1.84 times faster than that of a PVA cell with $P$ = 16 μm.

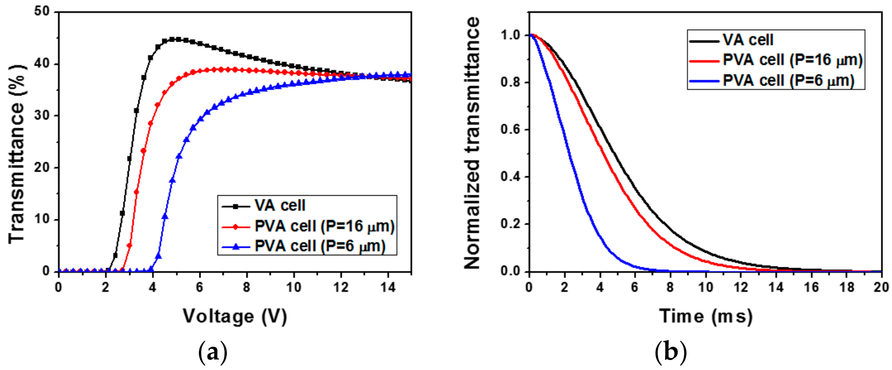


**Figure 5.** (**a**) Calculated voltage-transmittance curves and (**b**) temporal switching behavior during the turn-off process of PVA cells with the pitch *P* of patterned electrodes as a parameter. The spacing *L* between patterned electrodes was fixed at 2 μm.

Although the reduced pitch of the patterned electrodes is highly favorable for short response times, the reduced pitch could lead to a decrease in transmittance, which is a major tradeoff between the short response time and transmittance decrease in two-dimensionally confined LC cells [19–23]. In a VA-IPS cell using LCs with positive dielectric anisotropy, there is no change in the polar angle of the LC director at boundaries A and B, and the boundaries could be treated as virtual walls, as shown in Figure 6a,b [19]. At boundary A, where the vertical component of the electric field is dominant, the positive LC molecules remain vertically-aligned over a wider region than at boundary B where the in-plane component of the electric field is dominant, and a thicker virtual wall is formed. Therefore, in a VA-IPS cell, the transmittance significantly decreases as the pitch of the patterned electrodes decreases, which is caused by wide dead zones around boundary A, as shown in Figure 7. Conversely, a PVA cell using LCs with negative dielectric anisotropy exhibits a relatively high transmittance near boundary A as well as boundary B, as shown in Figure 6b. Unlike a VA-IPS cell where the LC molecules above the electrode are not switched, LC molecules with negative dielectric anisotropy around the center of the electrode are switched by the vertical component of the electric field in a PVA cell. In addition, patterned electrodes placed on each substrate generate a periodically dense electric field distribution in the longitudinal as well as the lateral direction, as shown in Figure 6b. As a result, the LC molecules are switched near the top substrate as well as near the bottom substrate, causing more LC molecules to be tilted downward near boundary A than those of a VA-IPS cell, resulting in a higher transmittance at the boundaries, as shown in Figure 6b. Therefore, a PVA cell shows little decrease in the transmittance despite the decrease in the pitch of the patterned electrodes, as shown in Figure 7. These results suggest that the response time of a PVA cell can be significantly reduced with little decrease in the transmittance by simply decreasing the pitch of the patterned electrodes.

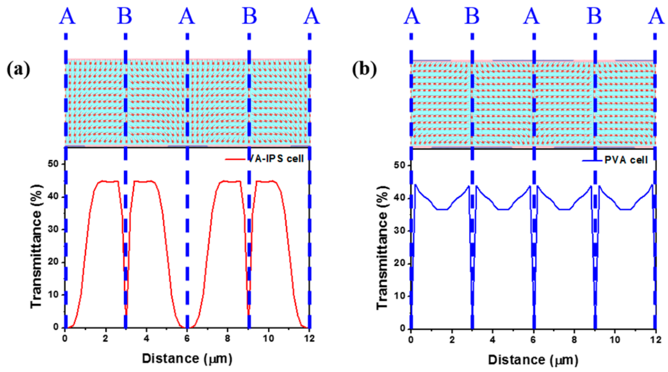


**Figure 6.** LC director orientations and transmittance distributions in (**a**) VA-IPS and (**b**) PVA cells.

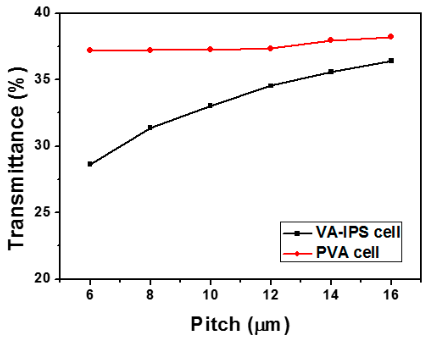


**Figure 7.** Calculated transmittances of VA-IPS and PVA cells as a function of patterned electrodes pitch *P*.

To account for the effect of misalignment on the turn-off time and transmittance, we calculated them as we increased the misalignment between the top and bottom patterned electrodes. As shown in Figure 8a, the dead zone is widened and the transmittance distribution becomes asymmetric as the misalignment is increased. Since the dead zone is widened, the reduction in transmittance is inevitable, as shown in Figure 8b. In a PVA cell with a pitch of 6 μm, the transmittance decreased by 11.4% from 38.22% to 34.3% when the PVA cell was misaligned by 0.5 μm, as shown in Figure 8b. The turn-off time increased by 2.96% from 3.72 ms to 3.83 ms under the same condition. These results show that a very accurate alignment of pixel electrodes is essential for practical applications of the proposed device.

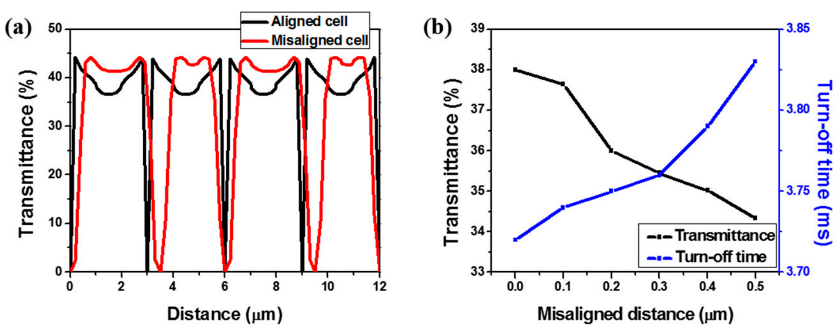


**Figure 8.** The effect of misalignment between the top and bottom patterned electrodes. (**a**) Transmittance distributions in an aligned cell and a cell misaligned by 0.5 μm; (**b**) Transmittance and turn-off time of PVA cells as functions of misalignment.

As demonstrated in previous studies, although three-terminal electrodes [24] and the formation of polymer networks made of liquid crystalline polymers in bulk [25] can be used to reduce the turn-off time of VA cells, some challenges still exist, such as a complicated manufacturing process, complicated drive scheme, low transmittance, and non-uniform distribution of residual polymer materials. Conversely, the fine patterning of pixel electrodes for a PVA cell is robust against such problems because the device does not require additional fabrication steps or complicated drive schemes.

## 4. Conclusions

We investigated the 2D confinement effect on the switching of vertically-aligned, negative LCs by an oblique electric field applied between the top and bottom patterned electrodes. When an electric field is applied to an LC cell, virtual walls form in the middle of the gaps between and at the center of the patterned electrodes. The LC molecules are confined not only by the two substrates but also by the virtual walls. Therefore, the turn-off time of a PVA cell can be reduced simply by decreasing the pitch of the patterned electrodes. The numerically calculated turn-off times obtained agree well with the 2D model. In contrast to a VA-IPS cell using LCs with positive dielectric anisotropy, a PVA cell using LCs with negative dielectric anisotropy exhibited a short response time with little decrease in the transmittance by the fine patterning of pixel electrodes. We believe that this device concept can be a potential candidate for realizing large, high-resolution, and high-frame-rate TV applications.

**Acknowledgments:** This work was supported by the National Research Foundation of Korea (NRF) grant funded by the Korea government (MSIP) (No. 2017R1A2A1A05001067).

**Author Contributions:** Yeongyu Choi, Tae-Hoon Choi, and Tae-Hoon Yoon planned the study. Yeongyu Choi wrote the manuscript; Yeongyu Choi and Tae-Hoon Choi conceived and designed the vertical alignment liquid crystal cell. Jae-Hyeon Woo and Byoung-Gyu Jeon performed the numerical simulations; Yeongyu Choi and Tae-Hoon Choi analyzed the data; Tae-Hoon Yoon supervised the analysis and co-wrote the manuscript. All authors discussed the results and also commented on the manuscript at all stages.

**Conflicts of Interest:** The authors declare no competing financial interests.

## References

1. Lee, J.H.; Park, K.H.; Kim, S.H.; Choi, H.C.; Kim, B.K.; Yin, Y. AH-IPS, superb display for mobile device. *SID Symp. Dig. Tech. Pap.* **2013**, *44*, 368. [CrossRef]
2. Luo, Z.; Wu, S.-T. OLED versus LCD: Who wins? *Opt. Photonics News* **2015**, *2015*, 19–21.
3. Ueda, N.; Okada, K.; Uchida, S.; Yamamoto, K.; Yamamoto, K.; Yoshida, H. Liquid crystal display with ultra-high resolution and super-fast response giving super reality to VR application. In Proceedings of the 23rd International Display Workshops, Fukuoka, Japan, 7–9 December 2016; pp. 281–284.
4. Yeh, P.; Gu, C. *Optics of Liquid Crystal Displays*; Wiley: New York, NY, USA, 1999.
5. Yang, D.-K.; Wu, S.-T. *Fundamentals of Liquid Crystal Devices*; Wiley: New York, NY, USA, 2007.
6. Chen, H.; He, J.; Wu, S.-T. Recent advances on quantum-dot-enhanced liquid crystal displays. *IEEE J. Sel. Top. Quantum Electron.* **2017**, *23*, 1900611. [CrossRef]
7. Schiekel, M.F.; Fahrenschon, K. Deformation of nematic liquid crystals with vertical orientation in electric fields. *Appl. Phys. Lett.* **1971**, *19*, 391–393. [CrossRef]
8. Lee, S.H.; Kim, S.M.; Wu, S.-T. Emerging vertical-alignment liquid-crystal technology associated with surface modification using UV-curable monomer. *J. Soc. Inf. Disp.* **2009**, *17*, 551–559. [CrossRef]
9. Kim, K.-H.; Song, J.-K. Technical evolution of liquid crystal displays. *NPG Asia Mater.* **2009**, *1*, 29–36. [CrossRef]
10. Kumar, P.; Jaggi, C.; Sharma, V.; Raina, K.K. Advancements of vertically aligned liquid crystal displays. *Micron* **2016**, *81*, 34–47. [CrossRef] [PubMed]
11. Takeda, A.; Kataoka, S.; Sasaki, T.; Chida, H.; Tsuda, H.; Ohmuro, K.; Sasabayashi, T.; Koike, Y.; Okamoto, K. A super-high image quality multidomain vertical alignment LCD by new rubbing-less technology. *SID Symp. Dig. Tech. Pap.* **1998**, *29*, 1077–1080. [CrossRef]
12. Kim, K.H.; Lee, K.H.; Park, S.B.; Song, J.K.; Kim, S.N.; Souk, J.H. Domain divided vertical alignment mode with optimized fringe field effect. *Proc. Asia Display* **1998**, *98*, 383–386.

13. Lee, B.-W.; Park, C.; Kim, S.; Jeon, M.; Heo, J.; Sagong, D.; Kim, J.; Souk, J. Reducing gray-level response to one frame; dynamic capacitance compensation. *SID Symp. Dig. Tech. Pap.* **2001**, *32*, 1260–1263. [CrossRef]
14. Song, J.-K.; Lee, K.-E.; Chang, H.-S.; Hong, S.-M.; Jun, M.-B.; Park, B.-Y.; Seomun, S.-S.; Kim, K.-H.; Kim, S.-S. DCC II: Novel method for fast response time in PVA mode. *SID Symp. Dig. Tech. Pap.* **2004**, *35*, 1344–1347. [CrossRef]
15. Kim, S.G.; Kim, S.M.; Kim, Y.S.; Lee, H.K.; Lee, S.H.; Lee, G.-D.; Lyu, J.-J.; Kim, K.H. Stabilization of the liquid crystal director in the patterned vertical alignment mode through formation of pretilt angle by reactive mesogen. *Appl. Phys. Lett.* **2007**, *90*, 261910. [CrossRef]
16. Nakanishi, Y.; Shibasaki, M.; Hanaoka, K.; Inoue, Y.; Tarumi, K.; Bremer, M.; Memmer, M.K.; Greenfield, S.; Harding, R. Liquid Crystal Display Device. U.S. Patent 7,169,449, 30 January 2007.
17. Lee, Y.-J.; Kim, Y.-K.; Jo, S.I.; Gwag, J.S.; Yu, C.-J.; Kim, J.-H. Surface-controlled patterned vertical alignment mode with reactive mesogen. *Opt. Express* **2009**, *17*, 10298–10303. [CrossRef] [PubMed]
18. Lee, S.H.; Kim, H.Y.; Park, I.C.; Rho, B.G.; Park, J.S.; Park, H.S.; Lee, C.H. Rubbing-free, vertically aligned nematic liquid crystal display controlled by in-plane field. *Appl. Phys. Lett.* **1997**, *71*, 2851–2853. [CrossRef]
19. Choi, T.-H.; Woo, J.-H.; Choi, Y.; Yoon, T.-H. Effect of two-dimensional confinement on switching of vertically aligned liquid crystals by an in-plane electric field. *Opt. Express* **2016**, *24*, 20993–21000. [CrossRef] [PubMed]
20. Choi, T.-H.; Oh, S.-W.; Park, Y.-J.; Choi, Y.; Yoon, T.-H. Fast fringe-field switching of a liquid crystal cell by two-dimensional confinement with virtual walls. *Sci. Rep.* **2016**, *6*, 27936. [CrossRef] [PubMed]
21. Choi, T.-H.; Choi, Y.; Woo, J.-H.; Oh, S.-W.; Yoon, T.-H. Electro-optical characteristics of an in-plane-switching liquid crystal cell with zero rubbing angle: Dependence on the electrode structure. *Opt. Express* **2016**, *24*, 15987–15996. [CrossRef] [PubMed]
22. Choi, T.-H.; Woo, J.-H.; Choi, Y.; Yoon, T.-H. Interdigitated pixel electrodes with alternating tilts for fast fringe-field switching of liquid crystals. *Opt. Express* **2016**, *24*, 27569–27576. [CrossRef] [PubMed]
23. Chen, H.; Tan, G.; Huang, Y.; Weng, Y.; Choi, T.-H.; Yoon, T.-H.; Wu, S.-T. A low voltage liquid crystal phase grating with switchable diffraction angles. *Sci. Rep.* **2017**, *7*, 39923. [CrossRef] [PubMed]
24. Kim, J.-W.; Choi, T.-H.; Yoon, T.-H. Fast switching of vertically aligned negative liquid crystals by optically hidden relaxation. *Liq. Cryst.* **2014**, *41*, 1212–1217. [CrossRef]
25. Baek, J.-I.; Kim, K.-H.; Kim, J.C.; Yoon, T.-H.; Woo, H.S.; Shin, S.T.; Souk, J.H. Fast switching of vertical alignment liquid crystal cells with liquid crystalline polymer networks. *Jpn. J. Appl. Phys.* **2009**, *48*, 056507. [CrossRef]